International Journal of Smart Grid and Clean Energy

Stability of DC micro-grid for urban railway systems

Sarah Nasr[a,b], Marc Petit[a], Marius Iordache[b], Olivier Langlois[b*]

[a] *GeePs | Group of electrical engineering – Paris UMR CNRS 8507, CentraleSupélec, Univ Paris-Sud, Sorbonne Universités, UPMC Univ Paris 06, 3-11 rue Joliot-Curie, Plateau de Moulon F-91192 Gif-sur-Yvette CEDEX*
[b] *Alstom Transport SA, 48 rue Albert Dhalenne, Saint-Ouen 93400, France*

Abstract

This paper studies the stability of a DC Micro-grid integrated in urban railway systems in order to recover trains braking energy. It is a green solution based on storing the excess of braking energy in a hybrid storage system and re-using it in non-railway applications such as auxiliary loads in a station or electric vehicles in proximity, which will increase the global energy efficiency. The risk of instability caused by constant power loads is detailed and solved using backstepping approach. It is shown that this problem can be solved by controlling the energy storage system.

Keywords: DC Micro-grid, stability, backstepping, railway, hybrid storage system

1. Introduction

In DC railway systems, there is a possibility to regenerate braking energy and to exchange it between trains. But in case of classic traction power supply consisting of diode-rectifiers with unidirectional power flow, there is no energy exchange with surrounding energy network and no possibility to integrate smart energy management system. Smart railway electrification will provide energy savings by accommodating all distributed generations (braking trains, renewable energy...) and storage systems (batteries, supercapacitors…). It will dynamically optimize the total power consumption and enhance power quality and system's efficiency. Railway system will no longer be a passive load consuming energy from the grid. It will take part of a larger smart grid and communicate with "non-railway" applications such as smart buildings, electrical vehicle charging stations… In this paper, the concept of recovering trains braking energy through a DC Micro-grid [1] is first presented. The stability of the system is then highlighted. In fact, when multi-sources and constant power loads (CPL) are connected to a DC Busbar, stability issues are faced. In the literature, this problem is usually analysed by small signal stability study which linearize the system around an operating point and makes it possible to use linear tools such as Bode and Nyquist diagrams, Routh-Hurwitz criterion [2]-[4]. However, railway braking energy is in the shape of unpredictable power peaks that can go up to 3MW in few seconds which make it not possible to define only one operating point to the system. Therefore, it is necessary to study the Micro-grid in its non-linear form. On the other hand, some have chosen damping filters with passive elements [3], [5]. This solution will increase the cost by over-sizing components (resistors, capacitors) which will also increase losses. Therefore, the backstepping approach [6] will be detailed. It will act on the control of the hybrid storage system and more precisely on the supercapacitor. It will stabilize the Micro-grid taking into consideration the dynamic evolution of the system.

2. Railway DC Micro-Grid

Nowadays, one of the challenges in railway systems is recovering the braking energy and avoiding

* Manuscript received April 30, 2015; revised August 11, 2015.
Sarah NASR. Tel.: +33-1-57061275; *E-mail address*: sarah.nasr@transport.alstom.com.
doi: 10.12720/sgce.4.3.261-268

losses. In fact, when an electric train brakes, it converts the mechanical kinetic energy to electrical energy and feeds it back into the source line (catenary or 3rd rail). This causes voltage increase at pantograph level. If another train is accelerating closely enough, the energy sent back to the catenary will be consumed by this train. In the opposite case, regenerated energy causes overvoltage which can damage the infrastructure. Therefore, when the voltage exceeds a threshold (*e.g.* 900V for 750V electrification system), the energy is burned in rheostats embedded in trains. The solution is to recover this energy before stimulating the rheostats through different technologies such as inverters, storage… The Railway DC Micro-grid, allows re-using the braking energy internally by the same operator but in different electrical applications, for example, lighting and escalators inside a metro station, electrical vehicles and buses parked outside the station... This eco-friendly solution will permit reducing energy losses, saving energy and thereby decreasing the total energy bill. In this paper, we will consider a scenario where the braking energy is used to charge electrical hybrid buses parked outside a metro station, thus enhancing the green multi-modal public transport deployment and improving the asset management of an urban transportation system.

2.1. Concept

Fig. 1(a) represents the global architecture of the DC Micro-grid. It consists of the following components:

- 900V DC busbar
- Two-level bidirectional inverter (4) connected to the LV power supply already available in the metro station
- DC/DC converters connecting the energy storage (2), railway system (1) and the hybrid buses (3) to the common DC busbar
- Hybrid energy storage device (5) containing supercapacitors (SC) and batteries.

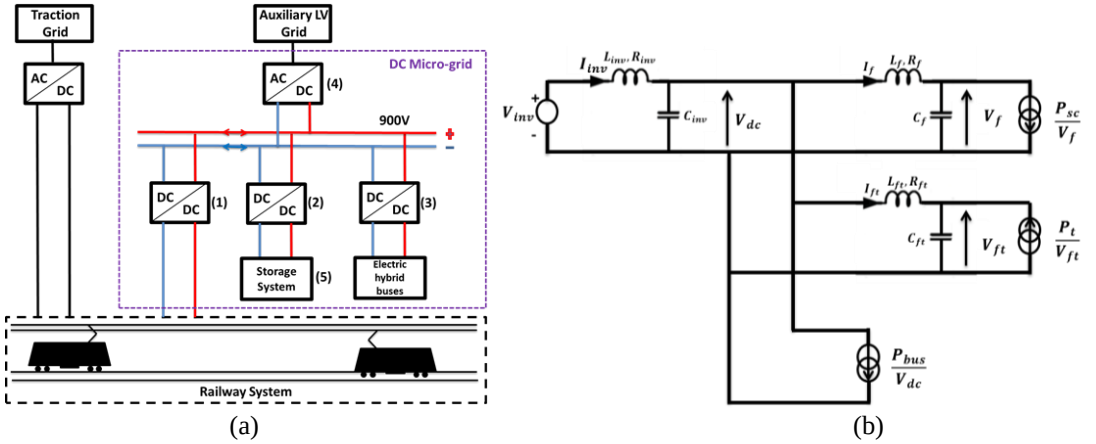

Fig. 1. The DC Micro-grid architecture: (a) global model and (b) simplified model.

The DC Micro-grid is connected to auxiliary low voltage grid. Therefore, a connection between both auxiliary and traction grids, usually separated in the case of diode rectifier substations, is possible through the DC Micro-grid. When a train brakes, the catenary (or third rail) voltage increases. Once the voltage exceeds a specific threshold, the converter (1) will recover the braking energy and inject it into the DC bus. This converter should be regulated to give priority to energy exchanging between trains. The second DC/DC converter (2) will store the energy and help reducing the DC busbar voltage. The AC/DC bidirectional inverter is used to regulate the DC bus voltage to avoid voltage peaks or drops.

2.2. Instability risk

In this use case, trains' braking energy is stored and then used to charge the electric hybrid buses.

These buses consume a constant power of 200 kW during 4-5 minutes. The problem of connecting a CPL is that its linear model behaves as a negative resistance (Fig. 2). It will then cause instability because it amplifies filters' dynamics in a resonant circuit. In the opposite case of Constant Power Source (CPS), its linear model behaves as positive resistance. It will damp the system dynamics caused by the input filter. The figures below show the behaviour of CPL and CPS [6].

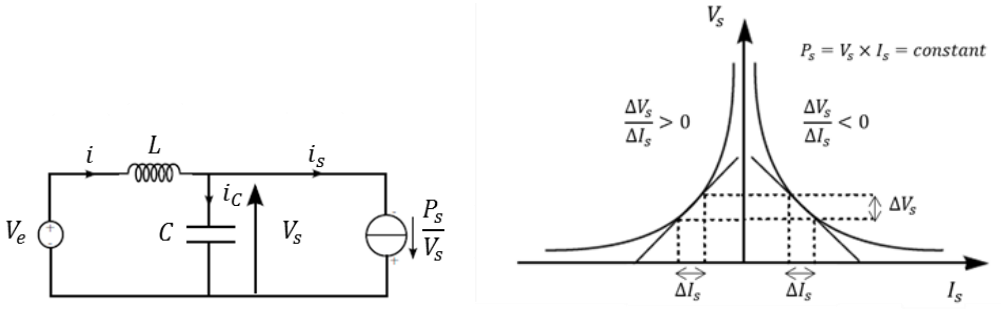

(a) (b)

Fig. 2. Linear model of a constant power load: (a) DC electrical network with CPL/CPS and (b) negative and positive impedance of CPL/CPS [6].

3. Backstepping Approach

3.1. DC Micro-grid modelling

In order to simplify the problem, the converters are represented by current sources operating in consumption/generation modes. In figure 1.b, the studied system is presented where V_{inv} represents the inverter's output voltage (V_{inv}=900V), P_{sc} the power absorbed by the hybrid storage system, P_t the braking power recovered by the trains and P_{bus} the constant power absorbed by the electric hybrid bus. The set of equations representing the system is given below. Note that V_{inv} and P_{bus} are constant, P_t is also considered as a constant because the system dynamics are much faster than the braking power variation. P_{sc} is the control command of the storage.

$$\begin{cases} L_{inv}\dfrac{dI_{inv}}{dt} = V_{inv} - V_{dc} - R_{inv}.I_{inv} \\ L_f\dfrac{dI_f}{dt} = V_{dc} - V_f - R_f.I_f \\ L_{ft}\dfrac{dI_{ft}}{dt} = V_{dc} - V_{ft} - R_{ft}.I_{ft} \end{cases} \quad \begin{cases} C_{inv}\dfrac{dV_{dc}}{dt} = I_{inv} - I_f - .I_{ft} - P_{bus}/V_{dc} \\ C_f\dfrac{dV_f}{dt} = I_f - P_{sc}/V_f \\ C_{ft}\dfrac{dV_{ft}}{dt} = I_{ft} + P_t/V_{ft} \end{cases} \tag{1}$$

Considering the vector X_0=[I_{inv0} , I_{f0} , I_{ft0} , V_{dc0} , V_{f0} , V_{ft0}] as an equilibrium point, equations (1) can be centred round X_0 with the following variable changes:

$$\begin{cases} x_1 = I_{inv} - I_{inv0} \\ x_2 = I_f - I_{f0} \\ x_3 = I_{ft} - I_{ft0} \end{cases} \quad \begin{cases} x_4 = V_{dc} - V_{dc0} \\ x_5 = V_f - V_{f0} \\ x_6 = V_{ft} - V_{ft0} \end{cases} \tag{2}$$

After replacing (2) in (1), the new equivalent system is given in (3) where the equilibrium point X_0 is the system's origin:

$$\begin{cases} L_{inv}\dot{x}_1 = -R_{inv}x_1 - x_4 \\ L_f\dot{x}_2 = -R_f x_2 + x_4 - x_5 \\ L_{ft}\dot{x}_3 = -R_{ft}x_3 + x_4 - x_6 \end{cases} \quad \begin{cases} C_{inv}\dot{x}_4 = x_1 - x_2 - x_3 + \dfrac{P_{bus}.x_4}{(x_4 + V_{dc0}).V_{dc0}} \\ C_f\dot{x}_5 = x_2 + \dfrac{P_{sc}.x_5}{(x_5 + V_{f0}).V_{f0}} \\ C_{ft}\dot{x}_6 = x_3 - \dfrac{P_t.x_6}{(x_6 + V_{ft0}).V_{ft0}} \end{cases} \tag{3}$$

3.2. System stabilization

After modelling the DC Micro-grid and centring the equations round the equilibrium point X_0, the backstepping control technique requires that equations describing the dynamics of the system (3) are presented in cascaded form. To achieve that, a change of variables is done as follows:

$$\begin{bmatrix} z_1 \\ z_2 \\ z_3 \\ z_4 \\ z_5 \\ z_6 \end{bmatrix} = \begin{bmatrix} L_{inv}x_1 + L_{ft}x_3 \\ C_{ft}x_6 \\ L_{inv}x_1 - L_{ft}x_3 \\ C_{inv}x_4 \\ L_f x_2 \\ C_f x_5 \end{bmatrix} \text{ and } \begin{bmatrix} z_{20} \\ z_{40} \\ z_{60} \end{bmatrix} = \begin{bmatrix} C_{ft}V_{ft0} \\ C_{inv}V_{dc0} \\ C_f V_{f0} \end{bmatrix} \text{ , with } \quad \frac{R_{ft}}{L_{ft}} = \frac{R_{inv}}{L_{inv}} \tag{4}$$

After applying (4), equations (3) can be expressed in the following cascaded form where 'u' is the backstepping command that will be added to the classic command P_{sc0} to ensure a global asymptotic stability:

$$\begin{cases} \dot{z}_1 = \varphi_1(z_1) + \psi_1 z_2 \\ \dot{z}_2 = \varphi_2(z_1, z_2) + \psi_2 z_3 \\ \dot{z}_3 = \varphi_3(z_1, z_2, z_3) + \psi_3 z_4 \end{cases} \quad \begin{cases} \dot{z}_4 = \varphi_4(z_1, z_2, z_3, z_4) + \psi_4 z_5 \\ \dot{z}_5 = \varphi_5(z_1, z_2, z_3, z_4, z_5) + \psi_5 z_6 \\ \dot{z}_6 = \varphi_6(z_1, z_2, z_3, z_4, z_5, z_6) + \psi_6 u \end{cases} \tag{5}$$

with,

$$\begin{cases} \varphi_1(z_1) = -R_{inv}.z_1/L_{inv} & \psi_1 = -\dfrac{1}{C_{ft}} \\ \varphi_2(z_1, z_2) = \dfrac{z_1}{2L_{ft}} - \dfrac{C_{ft}P_t z_2}{z_{20}(z_{20} + z_2)} & \psi_2 = -\dfrac{1}{2L_{ft}} \\ \varphi_3(z_1, z_2, z_3) = -\dfrac{R_{inv}}{2L_{inv}}(z_3 + z_1) - \dfrac{R_{ft}}{2L_{ft}}(z_3 - z_1) + \dfrac{z_2}{C_{ft}} & \psi_3 = -\dfrac{2}{C_{inv}} \\ \varphi_4(z_1, z_2, z_3, z_4) = \dfrac{1}{2L_{inv}}(z_3 + z_1) + \dfrac{1}{2L_{ft}}(z_3 - z_1) + \dfrac{C_{inv}P_{bus}z_4}{z_{40}(z_{40} + z_4)} & \psi_4 = -\dfrac{1}{L_f} \\ \varphi_5(z_1, z_2, z_3, z_4, z_5) = -\dfrac{R_f}{L_f}z_5 + \dfrac{1}{C_{inv}}z_4 & \psi_5 = -\dfrac{1}{C_f} \\ \varphi_6(z_1, z_2, z_3, z_4, z_5, z_6) = \dfrac{1}{Lf}z_5 + \dfrac{C_f P_{sc0} z_6}{z_{60}(z_{60} + z_6)} & \psi_6 = -\dfrac{C_f}{(z_{60} + z_6)} \end{cases}$$

where $R_{inv}, L_{inv}, R_f, L_f, R_{ft}, L_{ft}, C_{inv}, C_f$ and C_{ft} are constants characterizing the system; P_{bus} and P_t are

measurable, P_{sc0} is the classic command of the storage system and it is equal to: $P_{sc0} = P_t - P_{bus}$. The state vector presentation (5) will allow calculating the command 'u' by dividing the system to six cascaded subsystems S_i defined by the state vector [$z_1 \dots z_i$]. The backstepping method consists of calculating a positive-definite Lyapunov function V_i for each subsystem S_i. The global stability is then achieved by stabilizing each subsystem. The subsystem S_6 corresponds to the full system. Detailed calculus will be done for the first two subsystems; the rest can be done in the same manner. The command value of each S_i will be then directly given.

- Stabilization of subsystem S_1: $\dot{z}_1 = \varphi_1(z_1) + \psi_1 z_2$

For S_1, z_2 represent the input command of the subsystem. The command value z_1^* of z_1 is considered equal to zero. The state error ε_1 is given by:

$$\varepsilon_1 = z_1 - z_1^* \Rightarrow \dot{\varepsilon}_1 = \dot{z}_1 - \dot{z}_1^* = \varphi_1(z_1) + \psi_1 z_2 - \dot{z}_1^* \tag{6}$$

We consider the positive-definite Lyapunov function:

$$V_1 = \frac{1}{2L_{ft}} \varepsilon_1^2 \Rightarrow \dot{V}_1 = \frac{1}{L_{ft}} \dot{\varepsilon}_1 \varepsilon_1 = \frac{1}{L_{ft}} \varepsilon_1 (\varphi_1(z_1) + \psi_1 z_2 - \dot{z}_1^*) \tag{7}$$

S_1 is asymptotically stable if the derivation of V_1 is negative-definite. This condition is fulfilled by the following equation:

$$\varphi_1(z_1) + \psi_1 z_2 - \dot{z}_1^* = -k_1 e_1 \Rightarrow \dot{V}_1 = -k_1 e_1^2 < 0 \tag{8}$$

where $k_1 > 0$ is a parameter to be defined depending on the dynamic behaviour of S1.

In order to insure convergence to X_0, the command value z_2^* of z_2 should be equal to:

$$z_2^* = \frac{1}{\psi_1} (-\varphi_1(z_1) - k_1 e_1 + \dot{z}_1^*) \tag{9}$$

- Stabilization of subsystem S_2: $\{ \dot{z}_1, \dot{z}_2 \}$

For S_2, z_3 is the input command that will let the output z_2 equal to z_2^*. The state error vector is then:

$$\varepsilon_2 = z_2 - z_2^* \Rightarrow \dot{\varepsilon}_2 = \dot{z}_2 - \dot{z}_2^* = \varphi_2(z_1, z_2) + \psi_2 z_3 - \dot{z}_2^* \tag{10}$$

We consider the positive-definite Lyapunov function:

$$V_2 = \frac{1}{2C_{ft}} \varepsilon_2^2 + V_1 \Rightarrow$$

$$\dot{V}_2 = \dot{V}_1 + \frac{1}{C_{ft}} \dot{\varepsilon}_2 \varepsilon_2 = \frac{1}{L_{ft}} \varepsilon_1 (\varphi_1(z_1) + \psi_1(\varepsilon_2 + \dot{z}_2^*) - \dot{z}_1^*) + \frac{1}{C_{ft}} \varepsilon_2 (\varphi_2(z_1, z_2) + \psi_2 z_3 - \dot{z}_2^*) \tag{11}$$

S_2 is asymptotically stable if the derivation of V_2 is negative-definite. This condition is fulfilled by the following equation:

$$\frac{C_{ft}}{L_{ft}} \psi_1 \varepsilon_1 + \varphi_2(z_1, z_2) + \psi_2 z_3 - \dot{z}_2^* = -k_2 \varepsilon_2 \text{ with } k_2 > 0$$

The input command of S_2 is then:

$$z_3^* = \frac{1}{\psi_2}(-\frac{C_{ft}}{L_{ft}}\psi_1\varepsilon_1 - \varphi_2(z_1, z_2) + \dot{z}_2^* - k_2\varepsilon_2) \tag{12}$$

- Stabilization of subsystem S_3: $\{ \dot{z}_1, \dot{z}_2, \dot{z}_3 \}$

As for the previous subsystems, the input command z_4^* that will insure stability of S_3 is:

$$z_4^* = \frac{1}{\psi_3}(-\frac{L_{ft}}{C_{ft}}\psi_2\varepsilon_2 - \varphi_3(z_1, z_2, z_3) + \dot{z}_3^* - k_3\varepsilon_3) \text{ with } k_3 > 0 \tag{13}$$

- Stabilization of subsystem S_4: $\{ \dot{z}_1, \dot{z}_2, \dot{z}_3, \dot{z}_4 \}$

The input command z_5^* that will insure stability of S_4 is:

$$z_5^* = \frac{1}{\psi_4}(-\frac{C_{inv}}{L_{ft}}\psi_3\varepsilon_3 - \varphi_4(z_1, z_2, z_3, z_4) + \dot{z}_4^* - k_4\varepsilon_4) \text{ with } k_4 > 0 \tag{14}$$

- Stabilization of subsystem S_5: $\{ \dot{z}_1, \dot{z}_2, \dot{z}_3, \dot{z}_4, \dot{z}_5 \}$

The input command z_6^* that will insure stability of S_4 is:

$$z_6^* = \frac{1}{\psi_5}(-\frac{L_f}{C_{inv}}\psi_4\varepsilon_4 - \varphi_5(z_1, z_2, z_3, z_4, z_5) + \dot{z}_5^* - k_5\varepsilon_5) \text{ with } k_5 > 0 \tag{15}$$

- Stabilization of subsystem S_6: $\{ \dot{z}_1, \dot{z}_2, \dot{z}_3, \dot{z}_4, \dot{z}_5, \dot{z}_6 \}$

S_6 represents the Micro-grid. The input command 'u' that will insure the global stability of the system is:

$$u = \frac{1}{\psi_6}(-\frac{C_f}{L_f}\psi_5\varepsilon_5 - \varphi_6(z_1, z_2, z_3, z_4, z_5, z_6) + \dot{z}_6^* - k_6\varepsilon_6) \text{ with } k_6 > 0 \tag{15}$$

The Lyapunov function *V* of the system is:

$$V = \frac{1}{2L_{ft}}\varepsilon_1^2 + \frac{1}{2C_{ft}}\varepsilon_2^2 + \frac{1}{2L_{ft}}\varepsilon_3^2 + \frac{1}{2C_{inv}}\varepsilon_4^2 + \frac{1}{2L_f}\varepsilon_5^2 + \frac{1}{2C_f}\varepsilon_6^2 > 0 \tag{16}$$

The derivative of *V* is:

$$\dot{V} = -\frac{k_1}{L_{ft}}\varepsilon_1^2 - \frac{k_2}{C_{ft}}\varepsilon_2^2 - \frac{k_3}{L_{ft}}\varepsilon_3^2 - \frac{k_4}{C_{inv}}\varepsilon_4^2 - \frac{k_5}{L_f}\varepsilon_5^2 - \frac{k_6}{C_f}\varepsilon_6^2 < 0 \tag{17}$$

(16) and (17) ensures the asymptotic stability of the system around the origin X_0 which is calculated dynamically using Newton-Raphson method.

4. Simulation and Results

The simplified model of the DC Micro-grid shown in Fig. 1(b) is simulated using Matlab-Simulink.

The control command (15) is applied to the storage system. The k_i parameters used are:

$$k_1=50,\ k_2=30,\ k_3=13,\ k_4=8,\ k_5=300,\ k_6=10^{-5}.$$

The values of the electrical components of the DC Micro-grid are: C_f=0,041 F, C_{ft}=0,011 F, C_{inv}=3.532.10^{-4} F, L_f=10.12 µH, L_{ft} =9.45 µH, L_{inv} =11.9 µH, R_f=0.25 mΩ, R_{ft}=0.23mΩ, R_{inv} =0.29mΩ.

Fig. 3 shows profiles of the recovered braking power and the electric hybrid bus charging power. The first one increases from zero up to 1MW. The second one is 200kW constant power.

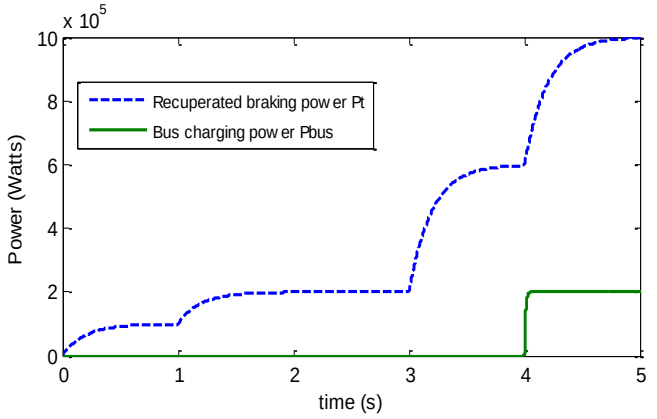

Fig. 3. Recovered power and bus charging power simulated profile.

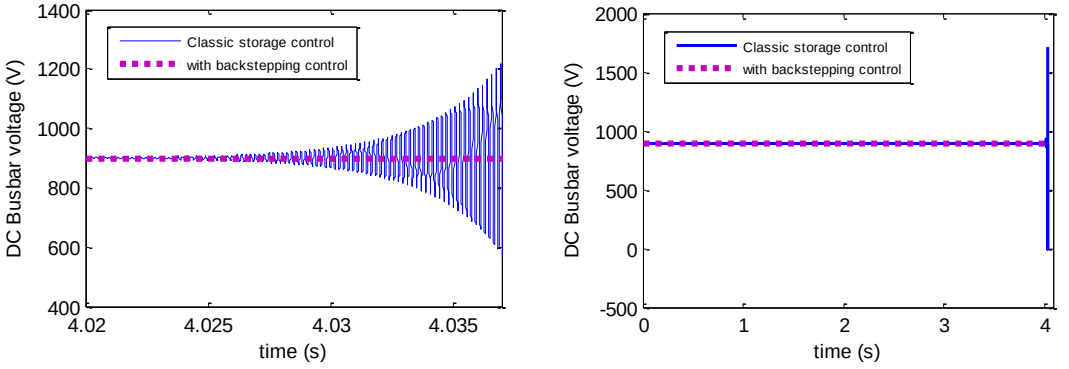

Fig. 4. DC busbar voltages for classic and backstepping controls.

Fig. 4 compares between the classic storage control ($P_{sc0} = P_t - P_{bus}$) and the one with backstepping control (P_{sc}=P_{sc0}+u). Note that the simulation with the classic control stops at time=4,035s for divergence reason. The backstepping control allowed stabilizing the system and by that the DC busbar voltage ($V_{dc} \cong 900V$).

5. Conclusion

In this paper, the concept of DC Micro-grid for urban railway systems was first presented. Its main role is to recover trains braking power, store it in a hybrid storage system and use this energy to charge electric hybrid buses with a constant power. The problem of instability that can be caused by a constant power load was then explained. A solution called backstepping approach was detailed and a comparison of simulation results between classic and backstepping controls proved that the backstepping control is capable of converging and stabilizing a low-damped system. The next step will be simulating

backstepping control on the complete DC Micro-grid with all the converters shown in Fig. 1(a).

References

[1] Nasr S, Iordache M, Petit M. Smart micro-grid integration in DC railway systems. Presented at: Innovative Smart Grid Technologies Conference Europe, 2014.

[2] Middlebrook RD. Input filter considerations in design and application of switching regulators. In: *Proc. IAS'76*, 1976:366–382.

[3] Godoy E, Coll. *Regulation Industrielle*. Paris: Dunod, 2007.

[4] Barruel F, Retiere N, Schanen JL, Caisley A. Stability approach for vehicles dc power network: application to aircraft on-board system. In: *Proc. IEEE 36th Power Electronics Specialists Conference*, June 2005:1163–1169.

[5] Erickson R. Optimal single resistors damping of input filters. In: *Proc. Applied Power Electronics Conference and Exposition, Fourteenth Annual IEEE*, Mar. 1999; 2:1073–1079.

[6] Hamache D, Fayaz A, Godoy E, Karimi C, Stabilization of a DC electrical network via backstepping approach. Presented at: 23rd International Symposium on Industrial Electronics, 2014.